Seventh Symposium on Salt, Vol. I 467–475 (1993)
Elsevier Science Publishers B.V., Amsterdam

Salt-Cavern Closure during and after Formation

F. Joseph Fischer[1], Bruce D. Light[2] and Paul R. Paslay[3]

[1]*Shell Development Company, Houston, Texas*
[2]*Shell Oil Company, Houston, Texas*
[3]*Techaid Corporation, Houston, Texas, USA*

ABSTRACT

An analysis over time of the behavior of salt caverns used for oil and gas storage is presented. The cavern and surrounding salt mass are modelled axisymmetrically and generalized plane strain is assumed for the vertical (axial) direction. The internal pressure acting on the cavern boundary is varied as a piecewise linear function of time to accommodate brine and other fluids within the cavern. The outer cylindrical boundary of the salt mass is either restricted from radial motion (multiple cavern array) or the radial stress is specified (single, isolated cavern). The present analysis predicts stresses and displacements within the salt mass as functions of time for either instantaneous or sequential cavern formation.

The disadvantage of other formulations compared to the one presented here is that instantaneous cavern formation has usually been assumed. In practice, the dissolutioning process occurs over a period of one year or longer while time constants for the salt are frequently of the order of several days. Earlier analyses have predicted that, typically, over one-half of the long-term cavern closure occurs during the first year. The small time constants and sizable first-year closure are inconsistent with the assumption of instantaneous cavern formation. Predictions using the present formulation, which tracks simultaneous, time-dependent dissolutioning and cavern closure, are compared with corresponding instantaneous cavern formation results.

INTRODUCTION

It is common practice to form caverns in salt domes for oil and gas storage. The caverns are often formed by solution mining; mechanical mining techniques are also used at shallow depths. The shape of these caverns, in most instances, can be approximated by slender circular cylinders with vertical axes. Typical diameters and lengths are 30 m and 300 m, respectively. The spacing between adjacent caverns in an array may be such that radial displacement of the salt at some radius is restrained by symmetry conditions. At the other extreme, the configuration may simulate an isolated cavern where it is reasonable to assume that the radial stress is fixed at a radius large compared to the cavern radius.

One commercially important characteristic of storage caverns is that following formation, the volume is reduced to some extent by creep closure. In some cases, most of this closure occurs within the first few years following formation. Volume reductions on the order of 40% over a one week period during low-pressure operations have been documented. Closure is caused by creep of the salt induced by the stress-state alterations associated with forming and subsequent pressurization of the cavern. This phenomenon has been studied extensively by Serata (1978) and, to a lesser extent, Fossum (1977). Serata has developed stress–strain equations to represent the salt behavior, and a rather comprehensive computer program which predicts cavern closure.

The purpose of the present work is to investigate sequential versus instantaneous cavern formation as well as to develop a computer program for preliminary design purposes. Serata's stress–strain equations are applied under the condition of generalized plane strain. Other constitutive models for salt behavior could likewise be utilized. The configuration studied is a cylinder of salt with a concentric hole, i.e., a thick-walled cylinder. Beginning from a uniform horizontal in situ stress-state present before the cavern is formed, the internal pressure on the cylinder is varied as a piecewise linear function of time. In general, the initial in situ horizontal and vertical stress components can be different. For the present model, the outer cylindrical boundary is either restricted from radial motion or the radial

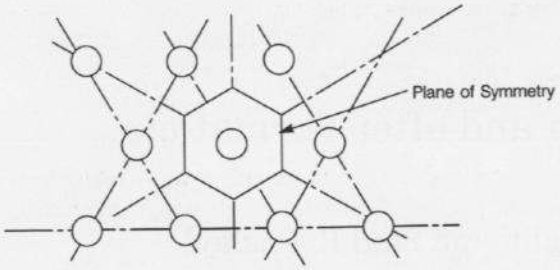

Fig. 1. Horizontal cross-section through an infinite array of hexagonally arranged caverns showing vertical planes of symmetry.

stress is specified. Restricted radial motion would correspond to this outer boundary being a "symmetry boundary" for the situation of multiple, closely spaced caverns as illustrated in Fig. 1. The total overburden load on the cylinder is maintained constant using the assumption of generalized plane strain. The salt dissolution rate at the inner radius is specified as a piecewise linear function of time. The program predicts stresses and radial displacements in the cylinder as functions of time.

This program provides useful predictions of cavern closure rates quickly and inexpensively for cases which do not require the complexity considered by other more comprehensive programs.

In addition, and of primary importance, this program has a feature not included in programs developed by Serata and others. For the present analysis, the dissolutioning rate is applied at each time step (sequential cavern formation). In Serata's program a full finite element block is the smallest dissolutioning step possible (instantaneous cavern formation). In Serata's published work he has usually accomplished the entire cavern dissolutioning process, which normally occurs over approximately one year, in one step. As some of the time constants associated with the material properties are the order of days, instantaneous cavern formation is a questionable assumption. Computed results are reported here to help evaluate the appropriateness of instantaneous cavern formation calculations.

MATERIAL DESCRIPTION

This analysis uses the material description formulation developed by Serata (1978). The salt is assumed to be homogeneous and isotropic with elastic, viscous, and plastic attributes. For mathematical simplicity, the strains, ε_{ij}, are separated into their deviatoric and mean normal parts as follows:

e_{ij} = ij component of reduced strain

$e_{ij} = \varepsilon_{ij} - \varepsilon_{kk} \cdot \delta_{ij}/3$

ε = mean normal strain = $\varepsilon_{kk}/3$.

Likewise, the stresses, σ_{ij}, are separated into their deviatoric and mean normal parts as follows:

S_{ij} = ij component of reduced stress

$S_{ij} = \sigma_{ij} - \sigma_{kk} \cdot \delta_{ij}/3$

σ = normal stress = $\sigma_{kk}/3$.

The strains are further separated into elastic, viscous and plastic parts. In addition, the plastic strains are written such that their mean normal value is zero, i.e., there is no plastic volume change. This separation is given below:

$e_{ij} = e_{eij} + e_{vij} + e_{pij}$

$\varepsilon = \varepsilon_e + \varepsilon_v$

where,

e_{eij} = ij component of elastic reduced strain,

e_{vij} = ij component of viscous reduced strain, and

e_{pij} = ij component of plastic reduced strain.

Serata's formulation has two states. These states are called the viscoelastic and viscoplastic states. The instantaneous value of the octahedral shear stress, τ_o, determines the state as follows:

Let τ_o = octahedral shear stress = $(S_{ij} \cdot S_{ji}/3)^{1/2}$

Then if $\tau_o < K_o$, or if $\tau_o = K_o$ and $\dot{\tau}_o < 0$, $\rightarrow$viscoelastic state

and if $\tau_o > K_o$, or if $\tau_o = K_o$ and $\dot{\tau}_o > 0$, $\rightarrow$ viscoplastic state.

The governing constitutive equations are different in each state. These constitutive equations yield the time rate of change of the strain. It is implicit in this formulation that all components of the elastic, viscous and plastic strains are continuous in time so that the strain is simply the integral of the strain rate.

Serata uses a spring-dashpot-slip element model to describe the mechanical behavior of salt. These models are shown in Fig. 2.

All results reported here are based on an infinite viscosity for the D_2 element. (Hence, K_2 can be arbitrary.) The effect of this choice is that the material does not experience viscous volume change.

The usual methods of continuum mechanics (see Timoshenko and Goodier, 1951, Prager and Hodge, 1951) can be applied to the above description of the material to deduce the following stress–strain equations:

Viscoelastic state

$$\dot{e}_{eij} = \dot{S}_{ij}/(2 \cdot G_1)$$

$$\dot{e}_{vij} = S_{ij}/(2 \cdot V_2) - \hat{e}_{vij} \cdot (G_2/V_2) \cdot e^{-G_2 \cdot (t-\hat{t})/V_2} - G_2/(2 \cdot V_2^2) \cdot e^{-G_2 \cdot t/V_2} \cdot \int_{t=\hat{t}}^{t} e^{G_2 \cdot t/V_2} \cdot S_{ij} \cdot dt$$

$$\dot{e}_{pij} = 0$$

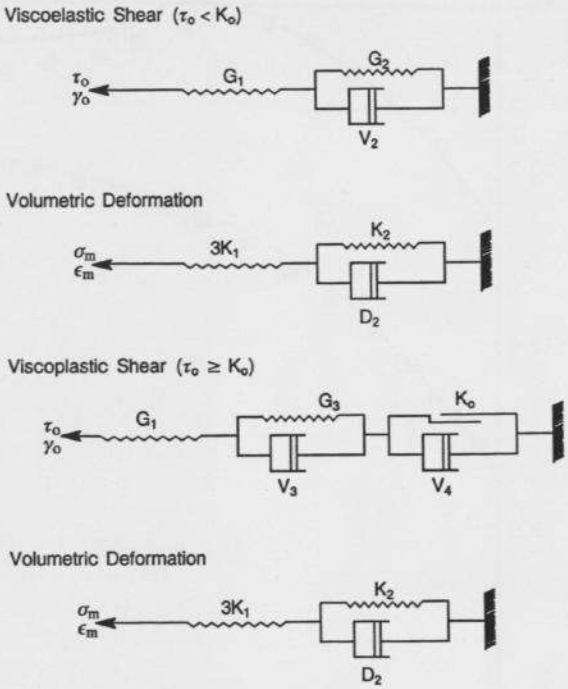

Fig. 2. Rheological model for salt proposed by Serata (1978) possessing both viscoelastic and viscoplastic flow behavior. (Permission from ASME.)

$$\dot{\varepsilon}_e = \dot{\sigma}/(3 \cdot K_1)$$

$$\dot{\varepsilon}_e = \sigma/D_2 - \hat{\varepsilon}_v \cdot (K_2/D_2) \cdot e^{-K_2 \cdot (t-\hat{t})/D_2}$$

$$- (K_2/D_2^2) \cdot e^{-K_2 \cdot t/D_2} \cdot \int_{t=\hat{t}}^{t} e^{K_2 \cdot t/D_2} \cdot \sigma \cdot dt$$

Viscoplastic state

$$\dot{e}_{eij} = \dot{S}_{ij}/(2 \cdot G_1)$$

$$\dot{e}_{vij} = S_{ij}/(2 \cdot V_3) - \hat{e}_{vij} \cdot (G_3/V_3) \cdot e^{-G_3 \cdot (t-\hat{t})/V_3}$$

$$- G_3/(2 \cdot V_3^2) \cdot e^{-G_3 \cdot t/V_3} \cdot \int_{t=\hat{t}}^{t} e^{G_3 \cdot t/V_3} S_{ij} \cdot dt$$

$$\dot{e}_{pij} = \left(1 - \sqrt{3} \cdot K_o/\sqrt{S_{\kappa l} \cdot S_{l\kappa}}\right) \cdot S_{ij}/(2 \cdot V_4)$$

$$\dot{\varepsilon}_e = \dot{\sigma}/(3 \cdot K_1)$$

$$\dot{\varepsilon}_v = \sigma/D_2 - \hat{\varepsilon}_v \cdot (K_2/D_2) \cdot e^{-K_2 \cdot (t-\hat{t})/D_2}$$

$$- (K_2/D_2^2) \cdot e^{-K_2 \cdot t/D_2} \cdot \int_{t=\hat{t}}^{t} e^{K_2 \cdot t/D_2} \cdot \sigma \cdot dt$$

In the above equations:

$$\hat{\xi} = \xi \,|_{t=\hat{t}}, \quad \xi = e_{vij} \text{ or } \varepsilon_v$$

The above formulation was used to develop equations appropriate for the numerical algorithm.

IDEALIZED SYSTEM DESCRIPTION

The system under investigation is symmetric about the vertical cylinder (cavern) axis. The cylinder of material is in a state of generalized plane strain. The ratio of the outer radius of the cylinder to the inner radius is, in general, much greater than one.

In order to predict the behavior of this thick-walled cylinder, the system is divided into NN-K cylinders. There are NN-1 cylinders initially and K are removed during dissolutioning. The i^{th} cylinder is bounded by r_i and r_{i+1}, and is illustrated in Fig. 3.

The configuration for a separate cylinder is defined by its axial strain, ε_z, which is the same for all separate cylinders, and its radial displacements U_{r_i} and $U_{r_{i+1}}$ measured from the initial, reference configuration.

The stresses σ_r, σ_θ and σ_z acting on a separate cylinder are assumed to be uniformly distributed on the normal faces upon which they act. Consequently, the stresses acting on the i^{th} cylinder shown in Fig. 3 are σ_{r_i}, $\sigma_{r_{i+1}}$, σ_{θ_i} and σ_{z_i}. The stress–strain equations for the i^{th} cylinder use average values of stress and strain.

Stress–strain, as well as radial and vertical force equilibrium equations for each cylinder, form the governing equations when the strains are written in terms of the displacements. This set of equations

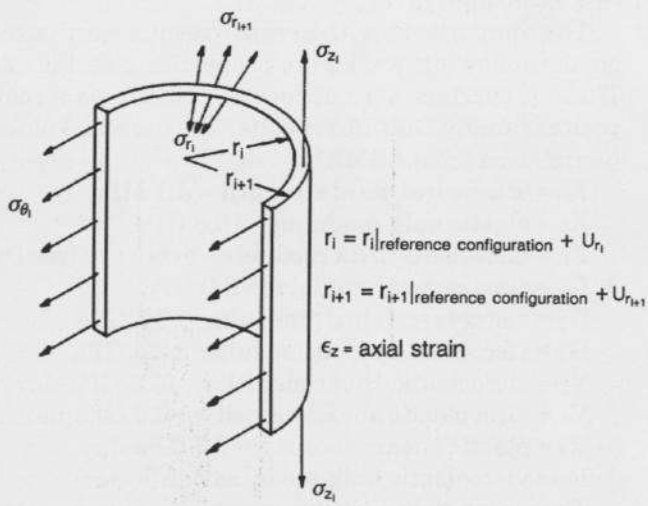

Fig. 3. Generic model element representation.

along with the boundary conditions form a set of (3 + 4 · (NN–K)) equations with as many unknowns. These equations have been programmed such that a numerical integration is accomplished. The program was prepared so that other constitutive relations could be introduced with minimum effort, however, the results presented here are restricted to the relations given previously. The radial thickness of the innermost element varies with time and may vanish during dissolutioning. Several elements are typically "dissolved" during cavern formation.

PROGRAM VERIFICATION

Numerical complexities, such as stability, are a concern in the current analysis; therefore, an attempt has been made to compare predictions made by this program with other known results. Three such computations were made. The computations were for (1) an elastic material, (2) an elastic-perfectly plastic (EPP) material, and (3) for a computation made using Serata's program. In the first two cases, the present model can be made to approximate the elastic and EPP materials by adjusting the material constants. For the elastic solution, the program matches a solution found in standard elasticity textbooks. For the EPP material the exact solution used for comparison is worked for a plane–strain condition while the program solves the problem for generalized plane–strain. So long as the axial strains from the present solution are small compared to the radial and tangential strains, the comparative results for the two problems are quite good. For the comparison with Serata's program, the material properties and boundary conditions are in agreement. Each of these numerical solutions was stable over the computation times considered.

The comparisons with Serata's results were based on the following weak salt properties (see Fig. 2). These properties were deduced by Serata as a composite of many Gulf Coast salts. They are as follows (permission from ASME):

K_o = octahedral yield strength = 4.1 MPa
K_1 = elastic bulk modulus = 13.8 GPa
K_2 = viscoelastic bulk modulus = arbitrary (see D_2)
G_1 = elastic shear modulus= 6.9 GPa
G_2 = viscoelastic shear modulus = 2.1 GPa
G_3 = viscoplastic shear modulus = 3.4 GPa
V_2 = viscoelastic shear viscosity =11.7 GPa-day
V_3 = viscoplastic shear viscosity = 6.9 GPa-day
V_4 = plastic shear viscosity = 9.7 GPa-day
D_2 = viscoelastic bulk modulus = infinite

The outer-to-inner radius ratio is four and the overburden stress is 17.2 MPa. The outer radius is fixed, corresponding to a multiple cavern configuration, and the pressure on the inner radius is rapidly decreased from the *in situ* value of 26.0 MPa to 9.0 MPa and held constant. These conditions correspond to a brine-filled cavern at a depth of 762 m with maximum excess lateral stress, i.e., $\sigma_r = 17.2 + 3K_o/\sqrt{2}$ MPa. Figure 4 shows a comparison of the radial and tangential stress after 1000 days. The results for radial stress agree rather well. Several points for the tangential stress do not agree well with the Serata prediction. However, all points are within approximately 5% of the curve. Figure 5 is a comparison of radial closure for the two computations. The two curves in Fig. 5 are similar but Serata's predicted closure is consistently higher than the current prediction.

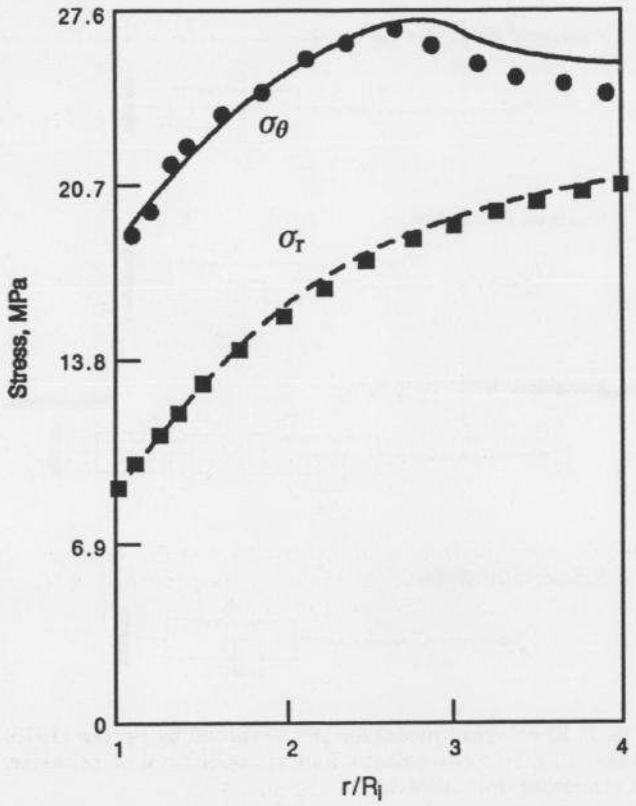

Fig. 4. Comparison of computed results (plotted as points) with Serata's program predictions (plotted as lines) for radial and tangential stresses after 1000 days. The brine-filled cavern depth and spacing, S/D, were 762 m and 4, respecively. Weak salt properties and the condition of maximum excess lateral stress, $\sigma_r = 17.2 + 3K_o/\sqrt{2}$ MPa, were assumed.

The above comparisons for three cases establish that the one-dimensional program is valid for estimating cavern behavior in the early stages of design. When a preliminary design has been completed, it is prudent to verify the design using a two-dimensional, axisymmetric model. As this one-dimensional program is inexpensive to use, it is of considerable value in making parameter studies.

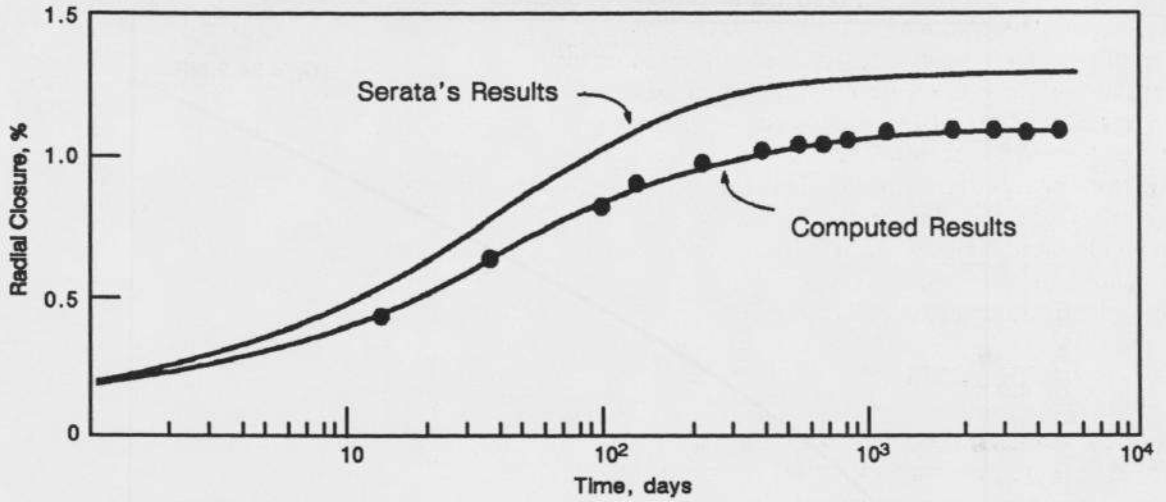

Fig. 5. Comparison of computed results with Serata's program predictions for inner radius closure. The brine-filled cavern depth and spacing, S/D, were 762 m and 4, respectively. Weak salt properties and the condition of maximum excess lateral stress, $\sigma_r = 17.2 + 3K_o/\sqrt{2}$ MPa, were assumed.

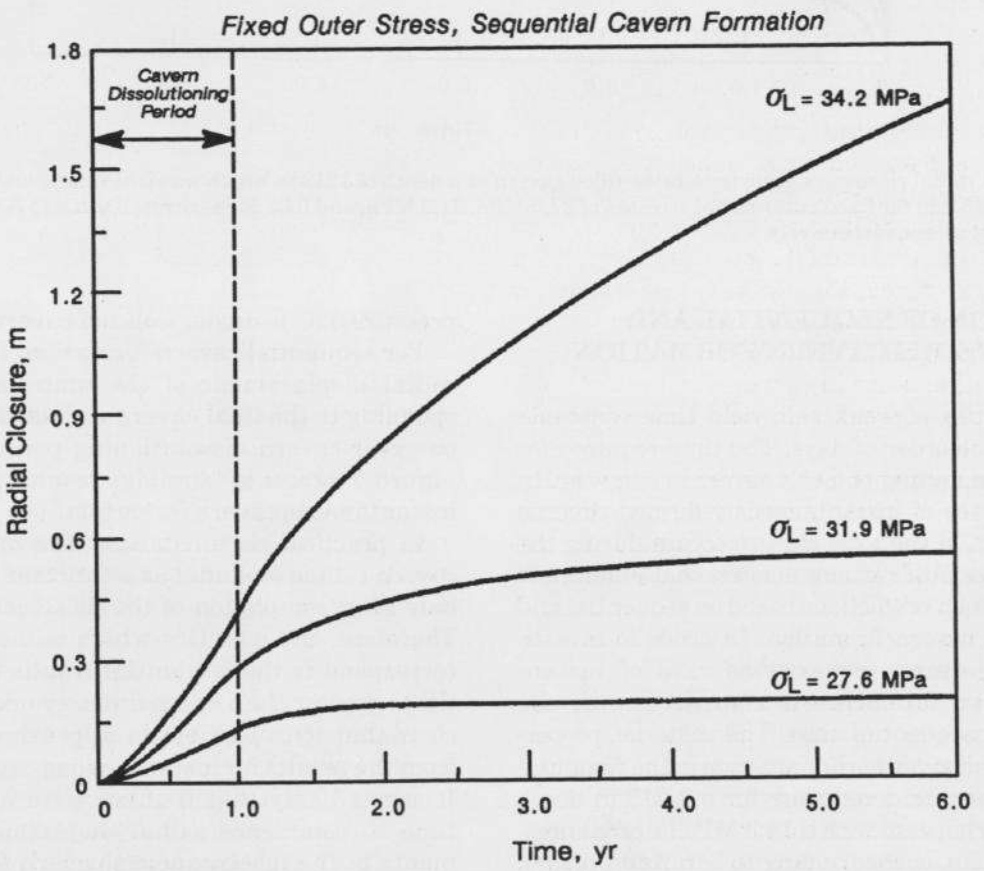

Fig. 6. Predicted radial closure vs. time for a brine-filled cavern at a depth of 1219 m, which was sequentially formed to a final radius of 15.2 m, for fixed outer radial stresses of 27.6 MPa, 31.9 MPa, and 34.2 MPa corresponding to 0, 1/2 and 3/4 times the excess lateral stress, respectively. The radial displacement was plotted at the material point which corresponds to the final cavern radius at the end of the one year cavern dissolutioning period.

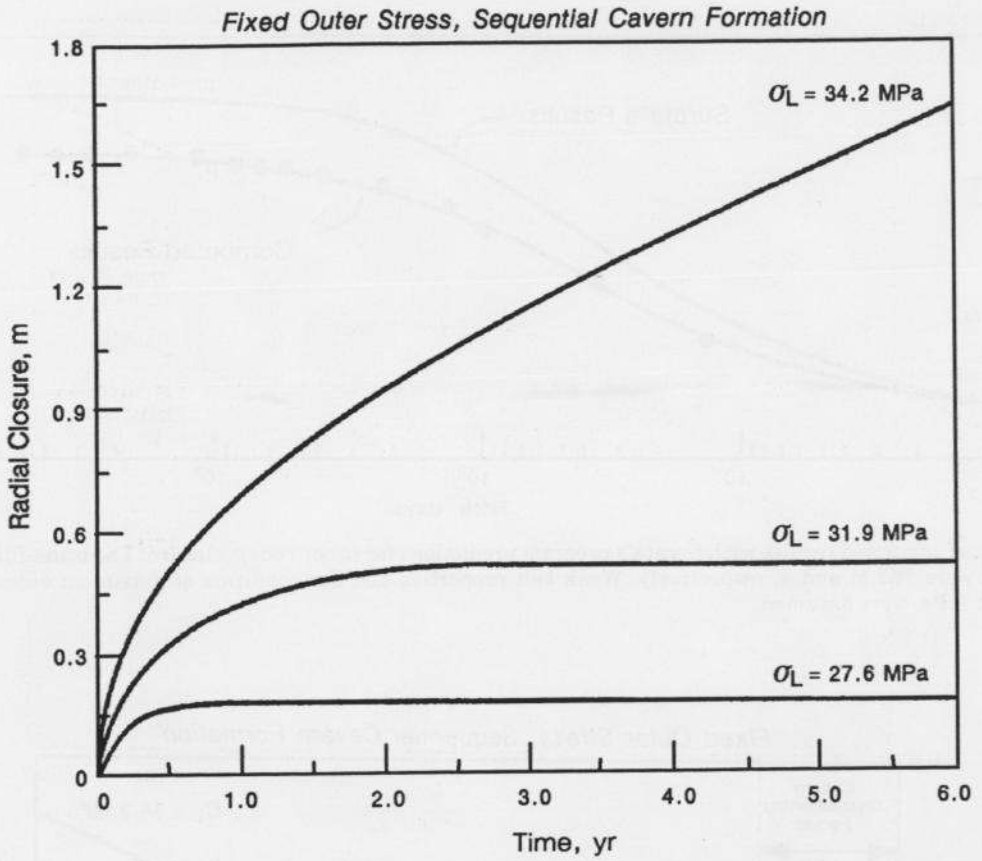

Fig. 7. Predicted radial closure vs. time for a brine-filled cavern at a depth of 1219 m which was instantaneously formed with an initial radius of 15.2 m for fixed outer radial stresses of 27.6 MPa, 31.9 MPa, and 34.2 MPa corresponding to 0, 1/2 and 3/4 times the excess lateral stress, respectively.

COMPARISON OF SEQUENTIAL AND INSTANTANEOUS CAVERN FORMATION

The properties of weak salt yield time constants which are of the order of days. The time required for typical solution mining of a salt cavern is one year. In general, analyses of instantaneously formed caverns predict 50–60% of the total closure occurs during the first year. These observations suggest that differences may exist between predictions based on sequential and instantaneous cavern formation. In order to investigate this conjecture, the extreme case of instantaneous cavern formation is compared with the corresponding sequential case. The material properties for weak salt given earlier are used in the computations. All cases considered were for a 1,219 m depth (27.6 MPa overburden) with a 14.3 MPa internal pressure (11.8 kPa/m, corresponding to saturated brine). The excess lateral stress, assumed before cavern formation, is either 0, 1/2, or 3/4 of $3K_o/\sqrt{2}$. This lateral stress, in other words, is specified as a fraction the value required to initiate *in situ* plastic flow. This illustrative example is for a constant external pressure, i.e., a single, isolated cavern.

For sequential cavern formation, Fig. 6 gives the radial displacement of the material point corresponding to the final cavern radius at the end of the one year cavern dissolutioning period versus time. Figure 7 presents "similar" results for the case of instantaneous cavern formation.

In practical circumstances, the measurement of cavern radius (volume) as a function of time is done only after completion of the dissolutioning process. Therefore, the quantity which is measured should correspond to the sequential results (see Fig. 6) for times greater than approximately one year. It is not clear that it is possible to approximate this curve from the results for instantaneous cavern formation. It seems likely that if there were an "equivalent" time to commence radial displacement measurements in the instantaneous cavern formation case, then this time would be less than the actual (sequential) formation time. In this event the sequential formation case could be bounded using the instantaneous cavity formation results. Figure 8 is a test of this hypothesis for the highest external pressure

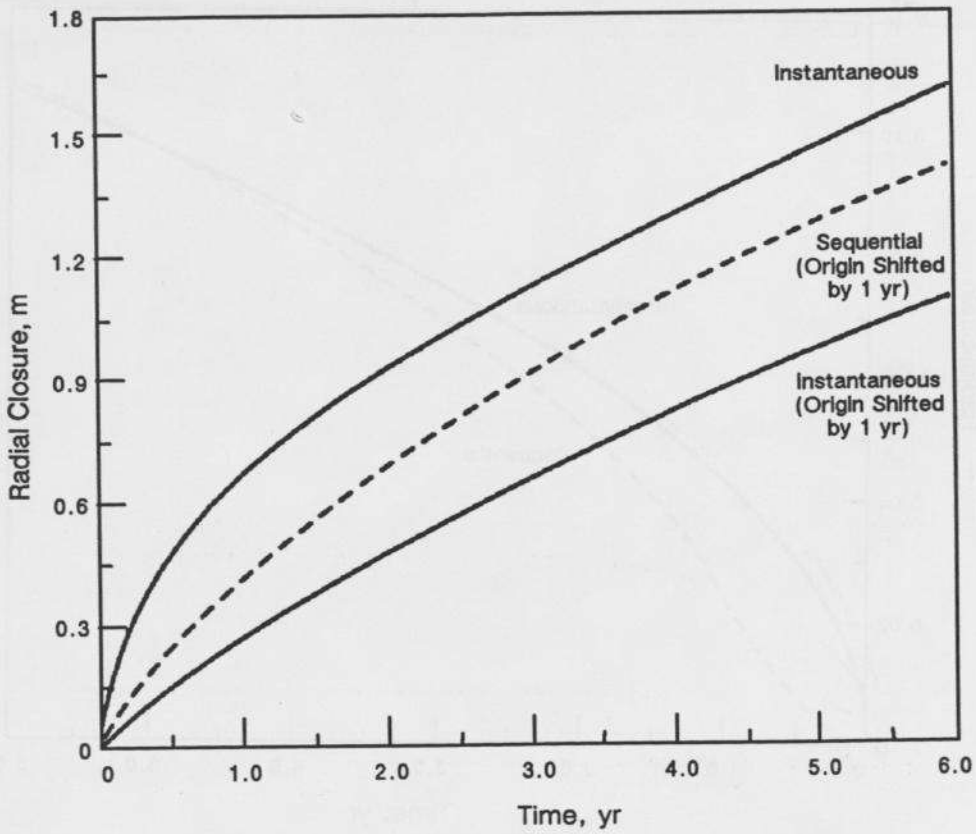

Fig. 8. Comparison of cavern radial closure vs. time between sequential and instantaneous cavern formation for the highest external pressure (radial compression) case given in Figs. 6 and 7.

case given in Figs. 6 and 7. The three curves appearing in Fig. 8 are (1) radial displacement for sequential cavern formation following dissolutioning, (2) the instantaneous cavern formation displacement as it appears in Fig. 6, and (3) the displacement given in Fig. 6 following a dissolutioning period of one year. The curves obtained from the instantaneous formation case are seen, in this case, to bound the sequential formation case as hypothesized. Unfortunately, the bounds are widely separated.

The radial strain history is of interest as it may be related to cavern wall failure by creep rupture during and after cavern dissolutioning or leaching (see Nair and Singh, 1974). It is, therefore, important to compare the radial strain histories for the instantaneous and sequential cavern formations. Figure 9 shows this comparison for the cases corresponding to the highest external pressure condition given in Figs. 6 and 7. The strain for the sequential case was plotted at the material point which corresponds to the final cavern radius at the end of the one year cavern dissolutioning period. The instantaneous cavern formation prediction of radial strain is seen to be considerably greater during the first several years than the sequential cavern formation prediction. Figure 10 is a plot of the mean radial strain at the cavern wall during leaching for the sequential cavern formation case in Fig. 9. Comparison of Figs. 9 and 10 shows that the cavern wall experiences radial strains during leaching which are comparable with cavern wall radial strains after leaching.

Fossum (1977) has investigated similar problems using a finite element computer program. His material stress–strain law formulation and problem configuration make direct comparison impossible. However, his conclusions do not contradict the results presented here.

CONCLUSIONS

A digital computer program has been developed to predict the mechanical behavior of salt dome storage caverns. This program is based on a one-dimensional (radial) approximation to the cavern. The following conclusions may be drawn from this work.

1. This program has been used to compare closure and radial strain at the material point which, after leaching, is on the cavity wall. Cases of instan-

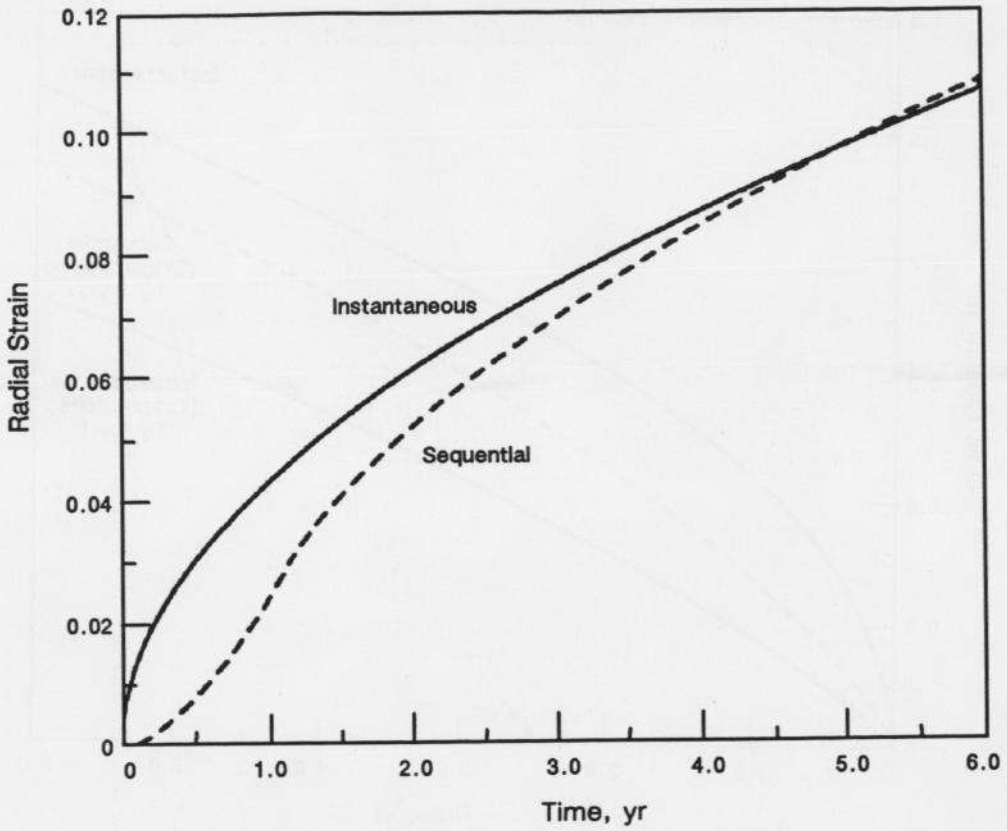

Fig. 9. Comparison of mean radial strain vs. time between sequential (final radius of 15.2 m) and instantaneous (initial radius of 15.2 m) cavern formation for a brine-filled cavern at a depth of 1219 m and a fixed outer radial stress of 34.2 MPa. The strain for the sequential case was plotted at the material point which corresponds to the final cavern radius at the end of the one year cavern dissolutioning period.

taneous and sequential cavity formation for common configurations have been compared. Although the long time (5 years) results are similar, the important practical comparison is for the behavior immediately following leaching and these results are quite different. The results of this comparison are:

(a) It is not possible to make an accurate determination of closure following leaching using an instantaneous cavern formation computation. A procedure is hypothesized in this work which uses the instantaneous cavity formation results to bound the post leaching sequential cavern formation closure. The procedure accomplishes the bounding for all cases considered here, but the bounds are widely separated (see Fig. 8).

(b) Comparison of the radial strain for instantaneous and sequential cavern formation shows that the histories are not similar except at long times. A criterion for cavern wall failure which is sensitive to radial strain history will require that the sequential cavern formation results be used, since both instantaneous strain rates and/or time integrations of strain histories are probably significant.

2. When compared with available two-dimensional (radial and axial) computer programs, this one-dimensional program executes very quickly and is thus inexpensive to use.

3. Comparison of this program's predictions with closed-form theoretical solutions and with predictions of Serata's program show that this program can be used for many preliminary design purposes. However, final design should be based on the best two-dimensional program available.

NOMENCLATURE

e_{ij}	ij component of reduced strain
ε_{ij}	ij component of strain
S_{ij}	ij component of reduced stress
σ_{ij}	ij component of stress
ε	mean normal strain, $\varepsilon^{kk}/3$
σ	mean normal stress, $\sigma^{kk}/3$
e_{eij}	ij component of elastic reduced strain
e_{vij}	ij component of viscous reduced strain
e_{pij}	ij component of plastic reduced strain

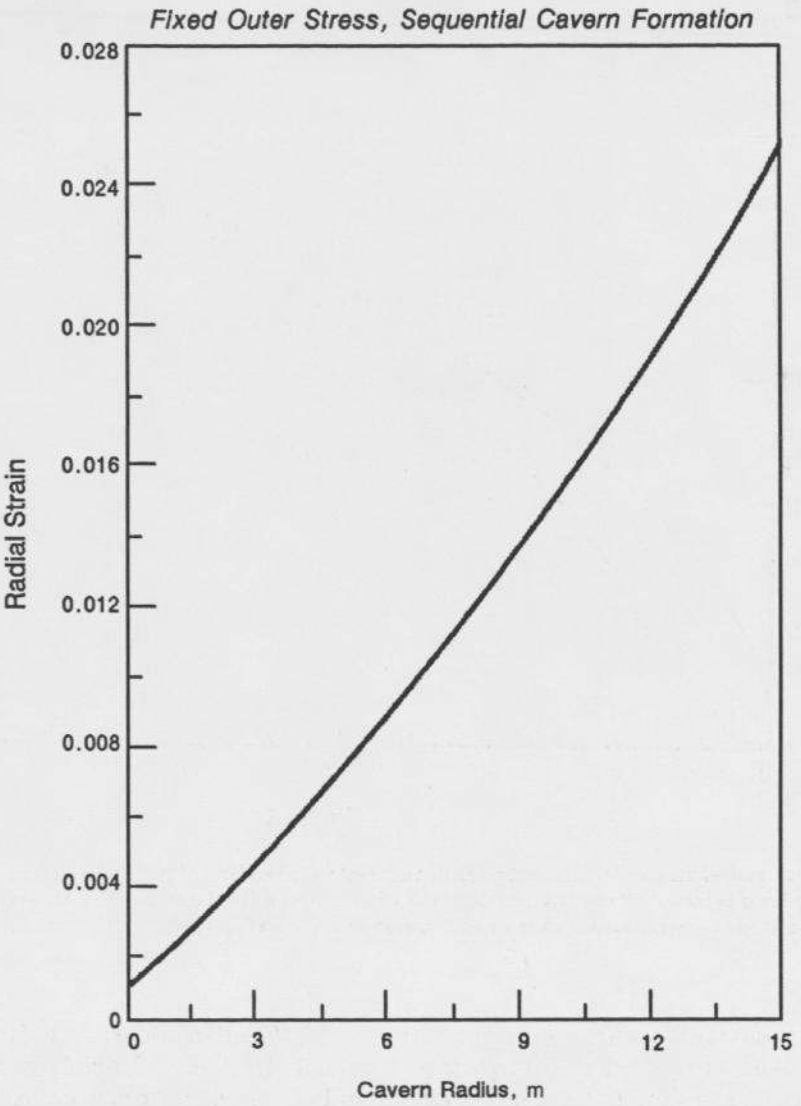

Fig. 10. Variation in mean radial strain at the cavern boundary vs. cavern radius during sequential cavern formation to a radius of 15.2 m for a fixed outer radial stress of 34.2 MPa.

τ_o Octahedral shear stress
K_o Octahedral shear strength
$\dot{\tau}_o$ Time rate of change of octahedral shear stress
$\dot{e}$ Time rate of change of reduced strain
t Time
$\sigma_r, \sigma_\theta, \sigma_z$ Radial, tangential, and vertical stresses, respectively
$\varepsilon_r, \varepsilon_\theta, \varepsilon_z$ Radial, tangential, and vertical strains, respectively
r, θ, z Radial, tangential, and vertical coordinates, respectively
U_r Radial displacement

REFERENCES

Fossum, A. F., 1977. On the structural behavior of progressively mined solution cavities in salt. J. Appl. Mech., 44: 565–570.

Nair, K. and Singh, R.D., 1974. Creep Rupture Criteria for Salt. In: A.H. Coogan (Editor), Fourth Symposim on Salt, Vol. 2. The Northern Ohio Geological Society, Inc., Cleveland, pp. 41–49.

Prager, W. and Hodge, P.G., Jr., 1951. Theory of Perfectly Plastic Solids. Wiley, New York, 264 pp.

Serata, S., 1978. Geomechanical Basis for Design of Underground Salt Cavities. American Society of Mechanical Engineers Publication Number 78-Pet-59.

Timoshenko, S. and Goodier, J.N., 1951. Theory of Elasticity, Second Edition. McGraw-Hill, New York, 506 pp.